ELECTROMAGNETIC PROPERTIES OF IMPACT-GENERATED PLASMA, VAPOR AND DEBRIS

DAVID A. CRAWFORD* AND PETER H. SCHULTZ**

*Computational Physics and Mechanics Dept. 9232, Sandia National Laboratories, Albuquerque, NM, 87185, USA;
**Department of Geological Sciences, Brown University, Providence, RI, 02912, USA.

Summary—Plasma, vapor and debris associated with an impact or explosive event have been demonstrated in the laboratory to produce radiofrequency and optical electromagnetic emissions that can be diagnostic of the event. Such effects could potentially interfere with communications or remote sensing equipment if an impact occurred, for example, on a satellite. More seriously, impact generated plasma could end the life of a satellite by mechanisms that are not well understood and not normally taken into account in satellite design. For example, arc/discharge phenomena resulting from highly conductive plasma acting as a current path across normally shielded circuits may have contributed to the loss of the Olympus experimental communications satellite on August 11, 1993. The possibility of significant storm activity during the Leonid meteor showers of November 1998, 1999 and 2000 (impact velocity, 72 km/s) has heightened awareness of potential vulnerabilities from hypervelocity electromagnetic effects to orbital assets. The concern is justified. The amount of plasma, electrostatic charge and the magnitude of the resulting currents and electric fields scale nearly as the cube of the impact velocity ($\propto v^{2.6}$). Even for microscopic Leonid impacts, the amount of plasma approaches levels that could be dangerous to spacecraft electronics. The degree of charge separation that occurs during hypervelocity impacts scales linearly with impactor mass. The resulting magnetic fields increase linearly with impactor radius and could play a significant role in our understanding of the paleomagnetism of planetary surfaces.

The electromagnetic properties of plasma produced by hypervelocity impact have been exploited by researchers as a diagnostic tool [1-3], invoked to potentially explain the magnetically jumbled state of the lunar surface [1-4] and blamed for the loss of the Olympus experimental communications satellite [5]. The production of plasma in and around an impact event can lead to several effects: (1) the plasma provides a significant perturbation to the ambient magnetic field via the electromagnetic pulse; (2) it supports the production of transient radiofrequency electromagnetic fields; (3) it charges ejected debris which, because of inertial separation, leads to significant electrostatic and magnetostatic field production; and (4) its high electrical conductivity provides a convenient path for discharge of the resulting high electrostatic fields. Effects (1) and (2) have been discussed by the authors elsewhere [1-3]. Effects (3) and (4) will be discussed here.

Typical studies of kinetic energy warheads focus on lethality as a function of impactor momentum or energy as they couple mechanically to the target. At high enough energies, however, additional physical processes come into play [6]. Vaporization plays an important role and a partially ionized plasma can form (Figure 1). Impact-generated plasma, charged debris and magnetic fields have been characterized by laboratory hypervelocity impact experiments and are shown to be more abundant when certain easily ionized materials (such as alkali metals) are used in either projectile or target [1-3,7].

DISCLAIMER

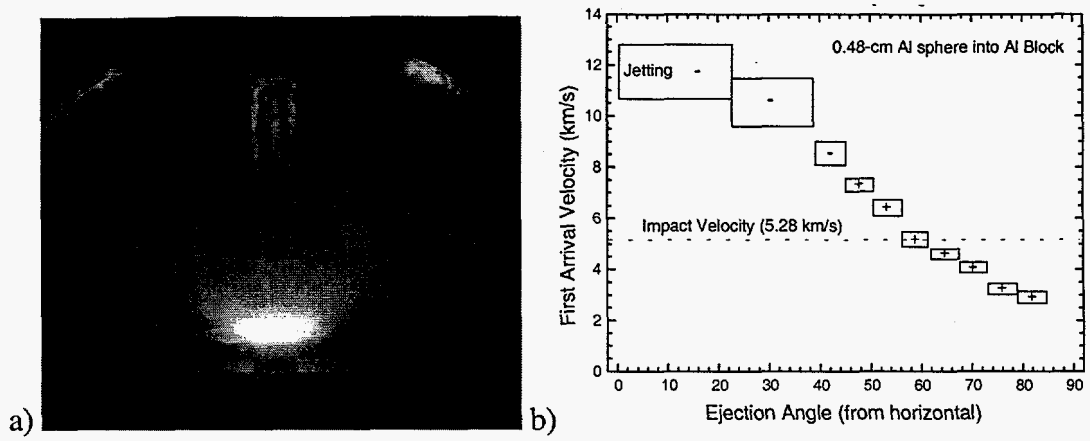

Fig. 1. a) Impact flash from 0.48 cm diameter aluminum sphere impacting vertically on an aluminum target block at 5.28 km/s (open shutter photograph). b) In this experiment, the target block was instrumented to measure departing charge and electric probes located in the arc seen at the top of the image (55 cm from the impact) measured the arrival of charged debris (traveling up to 12 km/s) jetting out from the point of impact. The +/- signs indicate the polarity of the initial arriving charge.

Dietzel *et al.* [7], studied the production of plasma from small particles in the hypervelocity impact regime. They used a parallel plate capacitor with 40 V/cm electric field to separate and measure the positive and negative constituents of the plasma for 10^{-15} to $5\text{x}10^{-10}$ g iron projectiles striking a tunsten target at1-40 km/s. The net charge liberated from an impact is zero, but, over the range of experimental conditions, the magnitude of the positive or negative charge carriers (Q) was found to have an approximate linear dependence on mass (m) and to have a strong dependence on impact velocity (v):

$$Q = 9\times10^{-9} m^{0.9\pm0.15} v^{2.75\pm0.4} \text{ C (SI units)} \quad (1)$$

At modest impact velocities (5 km/s), the level of ionization is low (typically 10^{-6}) [2]. At 40 km/s, however, the ionization level can be as much as 0.1 [7]. It is reasonable to suppose that at very high velocities the level of ionization and the amount of neutral vapor asymptotically approach a linear dependence on energy (v^2) and the fractional ionization will approach a constant value (<1) which is only dependent on impact geometry, projectile and target materials. Little evidence of this asymptotic behavior, however, is seen in the Dietzal *et al.* [7] data. With a reasonably conservative extrapolation of Equation (1) to Leonid encounter velocities (72 km/s), 10-20% of the plasma produced by Leonid impacts on spacecraft will be ionized and highly conductive.

In addition to plasma, a typical hypervelocity impact will produce melt and fragmental debris. Because electrons are much more mobile than ions, any debris in contact with plasma will typically acquire a negative charge. Inertial separation of the materials could then lead to separation of charge over macroscopic distances. This process, similar to static electrification that occurs in thunderclouds, can lead to substantial electric fields that are surprisingly easy to measure in the laboratory.

In experiments performed at the NASA Ames Vertical Gun Range, macroscopic charge separation during hypervelocity impact has been characterized for a variety of impactor and target geometries. The experiment depicted in Figure 2 was designed to measure the electrostatic field produced during a hypervelocity impact into a granular carbonate (dolomite) target. Aluminum plates were placed on the target plane radial to the impact point (Figure 2a). The voltage of each plate was measured with two digitizer channels: one to record strong, early-time signals (Figure

2b) the other to measure weak, late-time signals (Figure 2c). Each plate was terminated to ground via a 1 MΩ resistor.

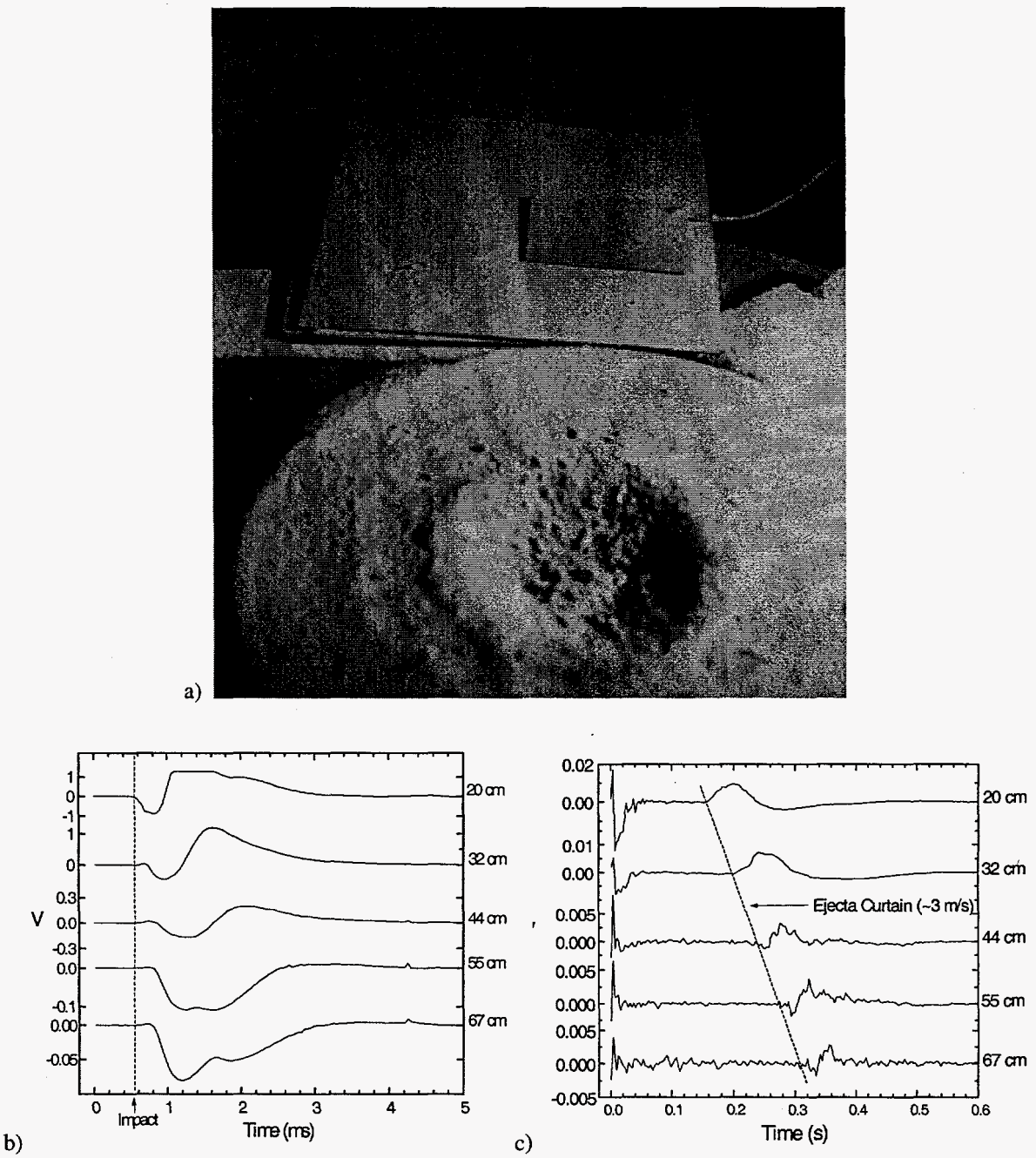

Fig. 2. Experiment to measure the electrostatic field produced by the impact of a ¼ inch Al projectile into a particulate carbonate target (impact velocity: 5 km/s, vertical). a) The impact crater (10 cm diameter) can be seen in the foreground and several of the plates located 20 and 32 cm from the impact are shown in the background. b) The electrostatic potential on a radial distribution of plates is shown with distance from the center of the impact crater indicated. c) At late time, charged ejecta land on the plates producing a discernable signal that allows ejecta curtain velocity to be measured.

The negative potential of the early time data in Figure (2b) and the positive charge of the ejecta landing on the plates at late time are consistent with early ejecta acquiring a negative charge and leaving behind a residual positive charge in the plasma, the transient cavity and material ejected at late time. The arrival time of the ejecta landing on the plates is consistent with an ejecta curtain velocity of 3 m/s (Figure 2c).

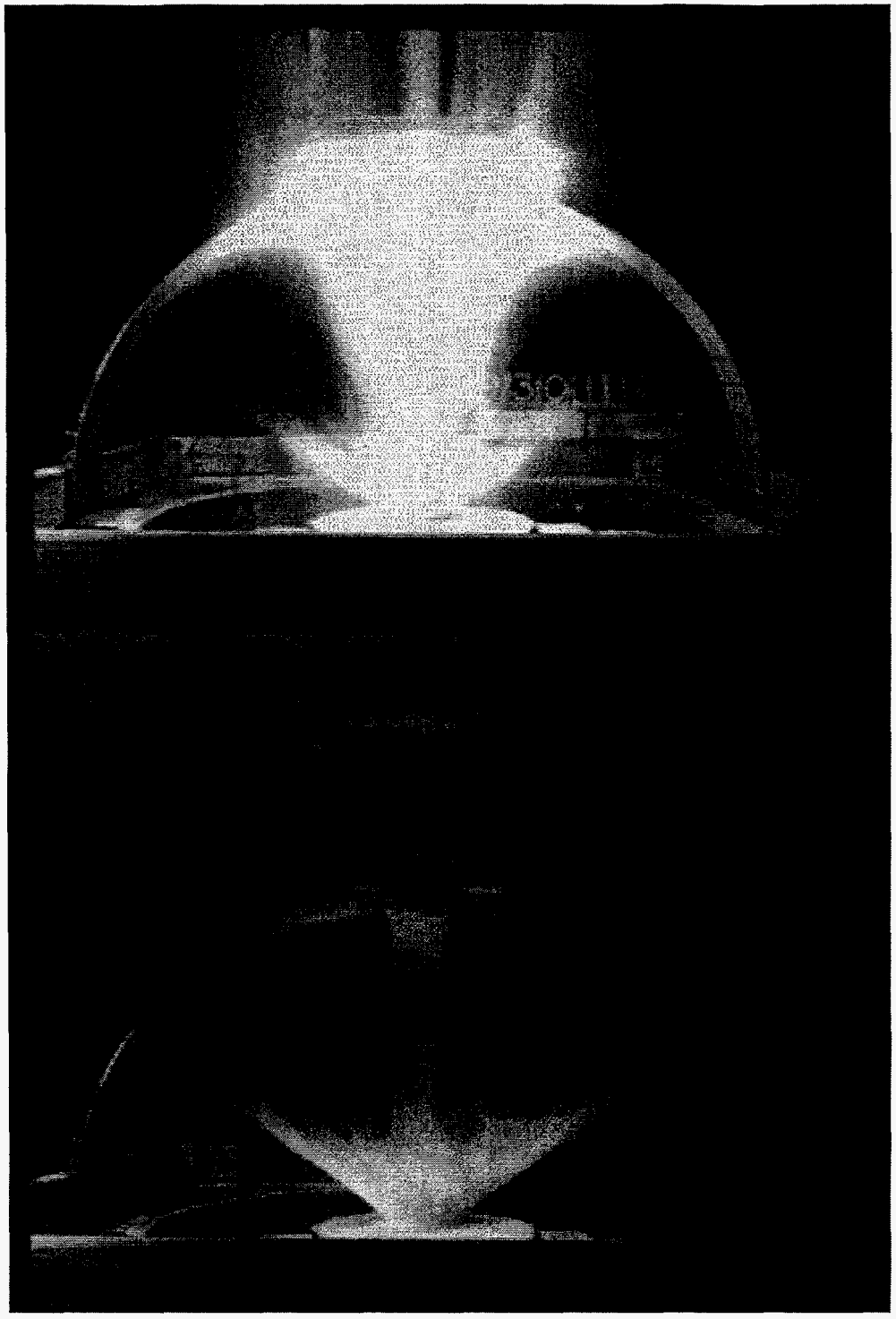

Fig. 3. Two movie frames from an experiment designed to measure the angular distribution of charge ejected from an impact in a particulate carbonate target. The projectile is a 0.48 cm aluminum sphere impacting at 5 km/s in an evacuated target chamber. The upper frame shows the luminescent impact-generated plasma impinging on the upper portion of an arc of 16 charge detection plates. The lower frame (2 ms later) shows ejecta hitting the arc at 35 degrees. The radius of the arc is 55 cm.

Unlike the experiment depicted in Figure 2, the experiment shown in Figure 3 was designed to directly measure the charge ejected at early time from impact craters formed by vertical hypervelocity impacts. The experiment contained an array of 16 aluminum plates used to detect the arrival of charge as a function of angle of ejection from the target surface. The arc of plates had a radius of 55 cm centered on the impact point. Each plate covered 5.5 degrees of arc and

was terminated with a 1 kΩ resistor. The resulting current traces are generally bimodal, showing negative or positive charge collection during certain times (Figure 4) A possible configuration of charge consistent with all the observations is illustrated in Figure 5.

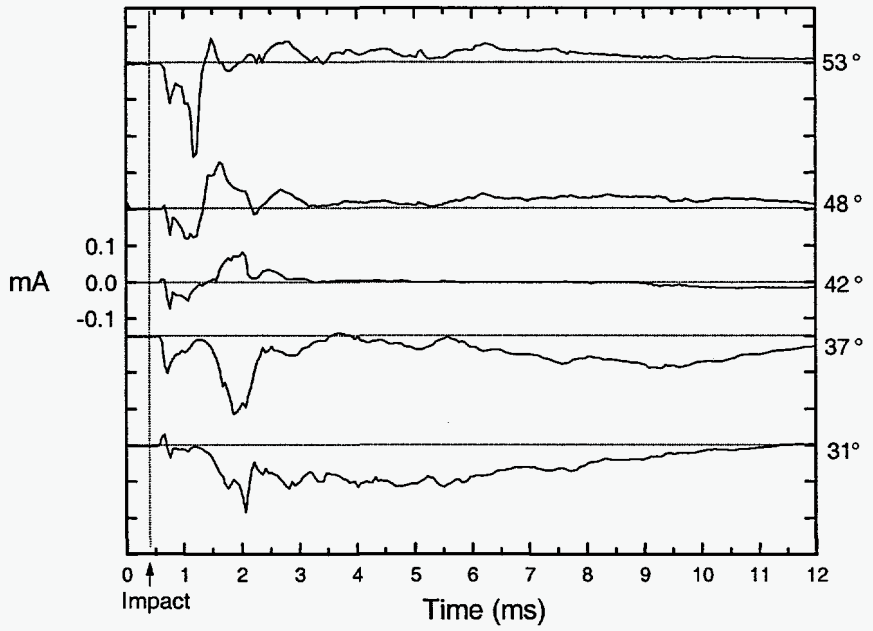

Fig. 4. Electric current collected by probes located 55 cm from the impact point of 0.48 cm Al sphere into granular carbonate target (impact velocity: 4.9 km/s). Each probe's ejection angle is indicated.

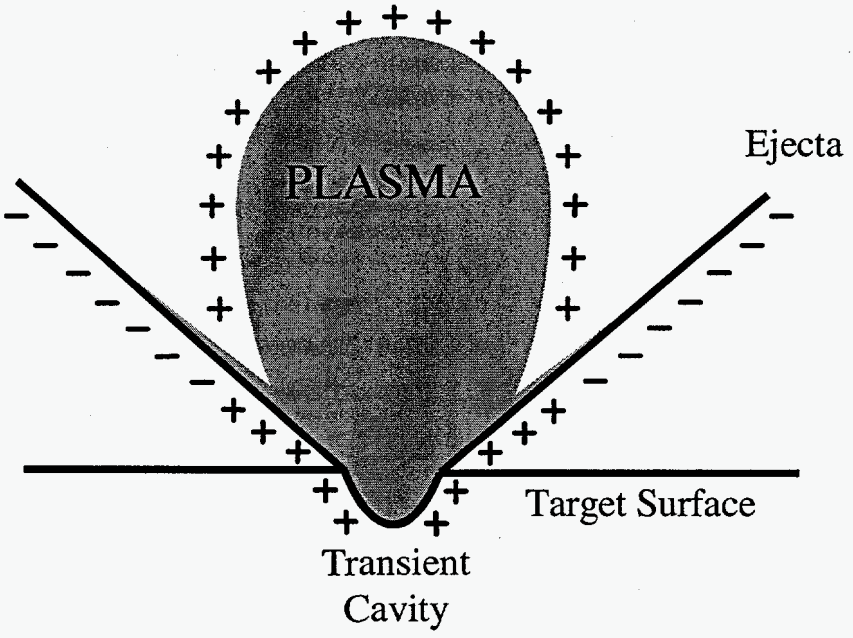

Fig. 5. Possible configuration of charge that explains the data.

Figure 6 shows the total, integrated charge collected at each range of solid angle for several impacts, demonstrating the consistency of the measurement and the dependence on impactor mass and velocity. Depending on ejection angle, the total charge is dominantly negative or positive. To demonstrate this, the positive and negative contributions to the total charge have been plotted separately in Fig. 6 (projecting above and below the horizontal lines respectively). A comparison with Fig. 3 suggests that early time ejecta is negatively charged and impact-generated plasma (moving to the top of Fig. 3) is positively charged.

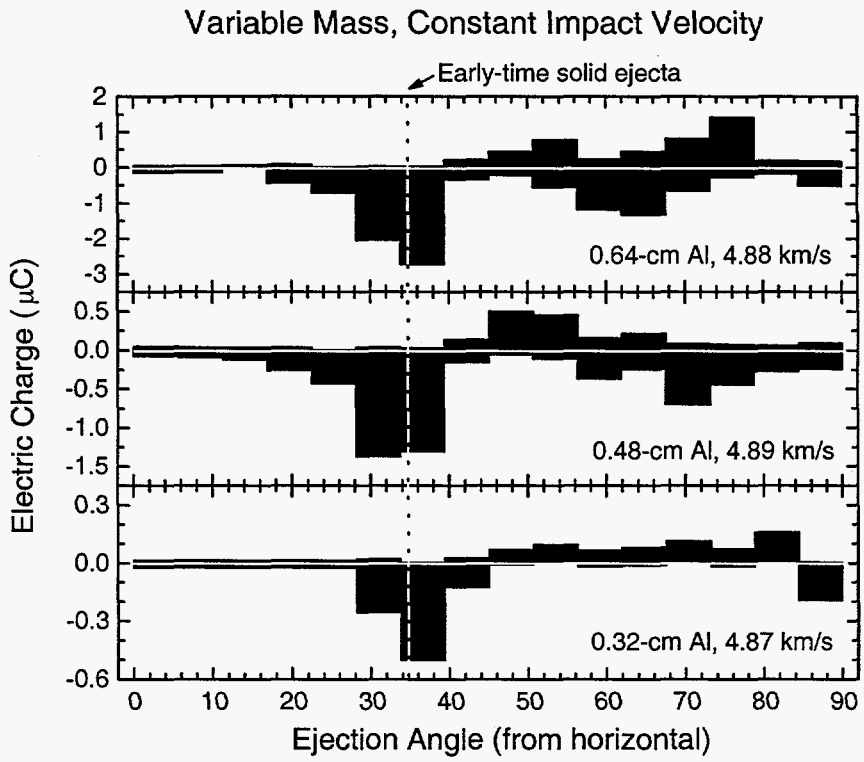

a)

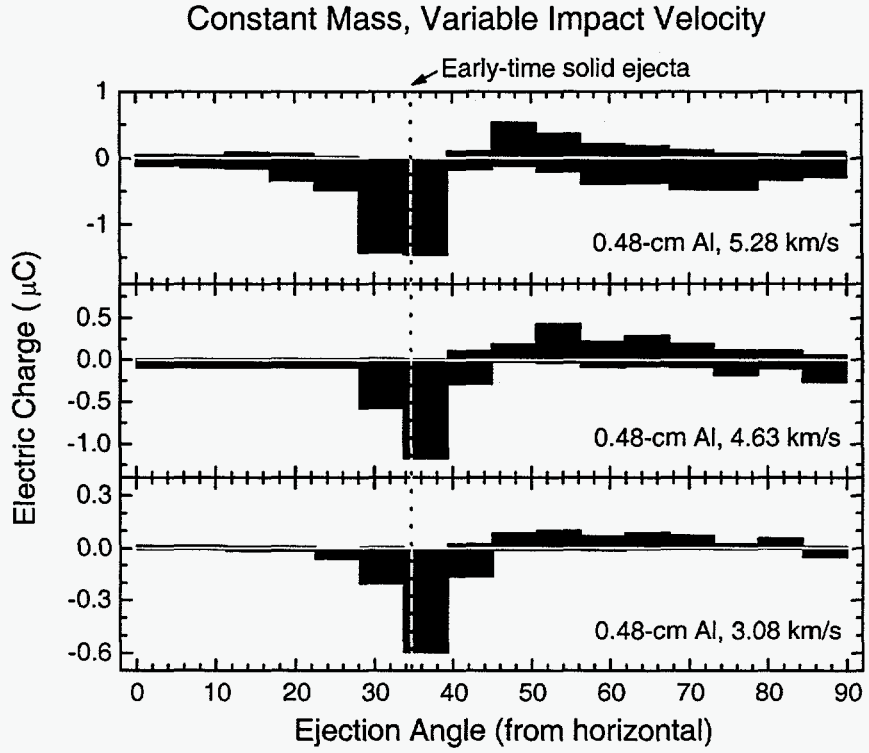

b)

Fig. 6. a) Total electric charge detected during impacts of 0.32, 0.48 and 0.64-cm Al projectiles into granular carbonate targets at 4.88 km/s. b) Total electric charged detected during 0.48-cm Al projectiles impacting at 3.08, 4.63 and 5.28 km/s. Location of early-time solid ejecta (measured from Fig. 3) is indicated.

In these experiments, dependence on impactor mass and velocity has been determined for a limited class of materials. Total charge separation is a function of impactor kinetic energy with a near linear dependence on mass and a velocity dependence of $v^{2.6}$ (Figure 7) comparable to the

dependence seen by Dietzel *et al.* [7]. This velocity dependence has strong implications for the degree of charge separation expected at Leonid encounter velocities (72 km/s) whereas the linear mass dependence has significant implications for the production of magnetostatic fields during planetary-scale impacts.

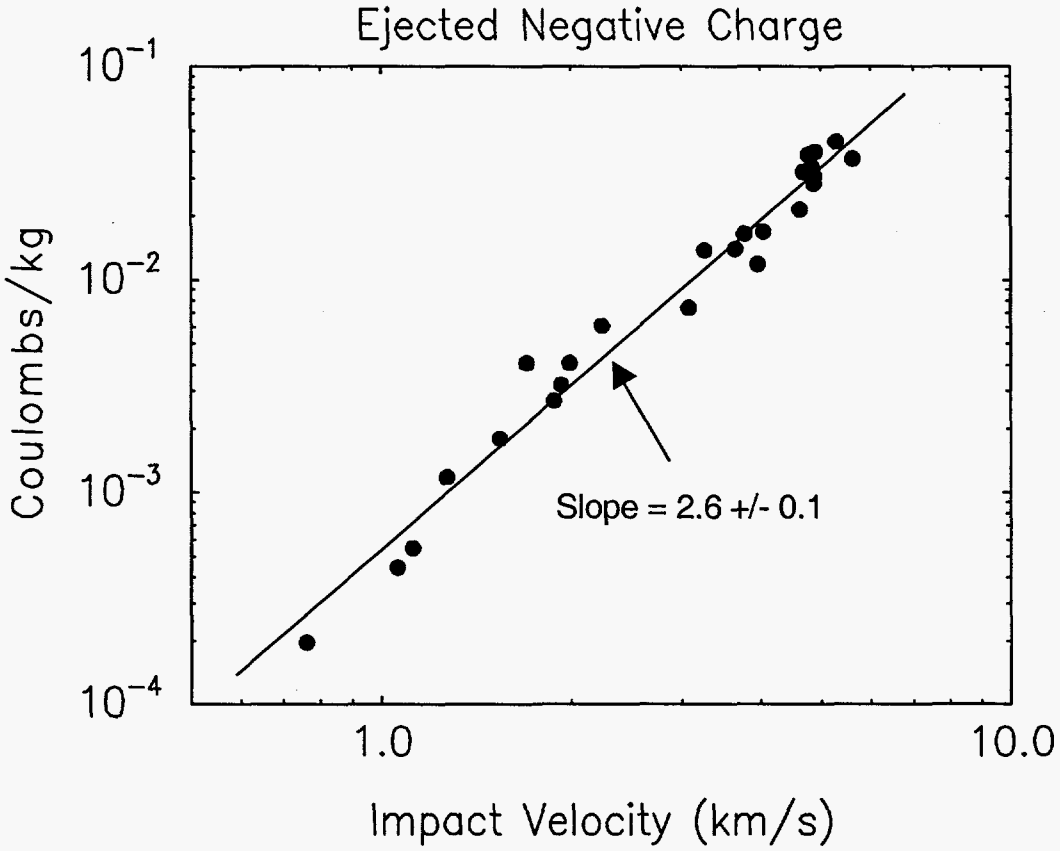

Fig. 7. Negative charge per unit mass ejected by impacts of spherical aluminum projectiles into granular carbonate (dolomite) targets vs. impact velocity.

Similar to Equation (1), the amount of charge separated by a macroscopic distance (ΔQ) can be expressed as functions of projectile mass (m) and impact velocity (v):

$$\Delta Q = 10^{-2} m \left(\frac{v}{3000} \right)^{2.6\pm0.1} \text{ C (SI units)} \qquad (2)$$

Table 1 compares the total charge (Q), the separated charge (ΔQ) and the degree of charge separation ($\Delta Q/Q$) for impact of 1 gram projectiles at different velocities:

Table 1. Electric charge as a function of impact velocity.

Velocity (km/s)	*Total Charge (Q) (Coulombs)*	*Separated Charge (ΔQ) (Coulombs)*	*Degree of Separation (ΔQ/Q)*
5	0.3	4×10^{-5}	1.4×10^{-4}
20	12	1.4×10^{-3}	1.2×10^{-4}
70	380	4×10^{-2}	9.5×10^{-5}

The extreme differences in projectile and target materials from which Equations (1) and (2) were determined make such comparisons problematic; nevertheless, they do provide some insight into the magnitude of charge separation that might occur. Even if only 10^{-4} of the total charge is

separated macroscopic distances, it is still significant for the production of electrostatic and magnetostatic fields.

The electric field produced by macroscopic charge separation during hypervelocity impacts is complicated by the contribution of electrostatic charge in the ejecta, the plasma and the transient cavity. To simplify the analysis and to provide a simple expression that exhibits the appropriate scaling behavior, we estimate the strength of the electric field by a spherical charge, $\pm \Delta Q$, centered at the impact point and expanding at a rate proportional to the impact velocity, v (as is approximately the case for expanding vapor or ejecta). If we make a measurement of the electric field at a distance x from the impact point, the magnitude of the electric field will last for a time, $\tau \propto x/v$. Using the data of Figure (2b) as a guide, we estimate $\tau \sim 20x/v$ in SI units. During this time, the electric field will have a magnitude:

$$E = \frac{3\Delta Q}{4\pi\varepsilon_0 x^2} = 2.7\times10^{10}\frac{\Delta Q}{x^2} \text{ Volts/m} \tag{3}$$

Charge separation will drive currents of magnitude:

$$I = \frac{\Delta Q}{\tau} = \frac{\Delta Q v}{20x} \text{ Amps,} \tag{4}$$

and magnetic fields with magnitude:

$$B = \mu_0 \frac{I}{2\pi x} = 10^{-8}\frac{\Delta Q v}{x^2} \text{ Tesla,} \tag{5}$$

will be produced. Substituting Equation (2) into Equations (3-5), we find:

$$E = 0.24\frac{mv^{2.6\pm0.1}}{x^2} \text{ Volts/m,} \tag{6}$$

$$I = 5\times10^{-13}\frac{mv^{3.6\pm0.1}}{x} \text{ Amps,} \tag{7}$$

$$B = 9\times10^{-20}\frac{mv^{3.6\pm0.1}}{x^2} \text{ Tesla.} \tag{8}$$

For naturally occurring impacts on planetary surfaces, the distance at which the electric and magnetic fields are significant is often proportional to the size (r_c) of the resulting impact crater. Because $x \propto r_c \propto r$ and $m \propto r^3$, the electric and magnetic fields of interest would tend to scale linearly with impactor radius (r). In the laboratory and during impacts on spacecraft, however, the location of the measurement is governed by other things and it is useful to maintain an independent measurement location (x).

Table 2 shows estimates for the magnitude and duration of the electric field, electric current and magnetic field for several cases: 1) a laboratory experiment (m=2x10^{-4} kg, x=0.5 m, v=5 km/s), 2) a Leonid meteoroid (m=10^{-7} kg, x=1 m) striking a spacecraft at 72 km/s, 3) a small meteoroid (m=1 kg, x=3 m) striking the Moon at 15 km/s and 4) a 1 km asteroid (m=10^{12} kg, x=100 km) striking a planetary surface at 20 km/s.

Table 2. Electromagnetic properties of representative impacts.

	τ (sec.)	E (Volts/m)	I (Amps)	B (Tesla)
1) Laboratory	$2x10^{-3}$	$8x10^{5}$	$4x10^{-3}$	10^{-9}
2) Leonid Meteoroid	$3x10^{-4}$	10^{5}	0.02	10^{-8}
3) Small Meteoroid	$4x10^{-3}$	$2x10^{9}$	180	10^{-5}
4) 1 km Asteroid	100	$4x10^{12}$	$2x10^{10}$	0.03

Except for the electric field, which was not measured, the laboratory numbers here agree well with experiments performed as part of this study (Figure 4) once a solid angle correction is performed. The magnetic field value agrees well with previous studies of fields observed during hypervelocity impacts [3].

A microscopic Leonid meteoroid striking a spacecraft at 72 km/s has the potential of inducing stronger electrical currents than those seen during typical macroscopic impact experiments. Discharges will drive higher currents in inverse proportion to their duration. A three microsecond discharge during a Leonid impact, for example, can drive a brief two amp current before exhausting the available charge.

The electric fields shown here are significant. By way of comparison, air typically becomes conducting at about $3x10^{6}$ V/m although the small amount of air that could support a discharge would interfere substantially with charge separation at the laboratory scale (Figure 8). Even without the presence of air, the electric field of large asteroid impacts may still be self limiting. In the presence of 10^{10} V/m electric fields, sub-micron dust grains, with just a few excess electrons of charge, will acquire accelerations of several km/s^2. Perhaps electrostatically-driven dust transport may occur during impacts on airless bodies. The resulting 'dust discharges' would tend to limit the buildup of charge and the strength of the electric and magnetic fields to some saturation level.

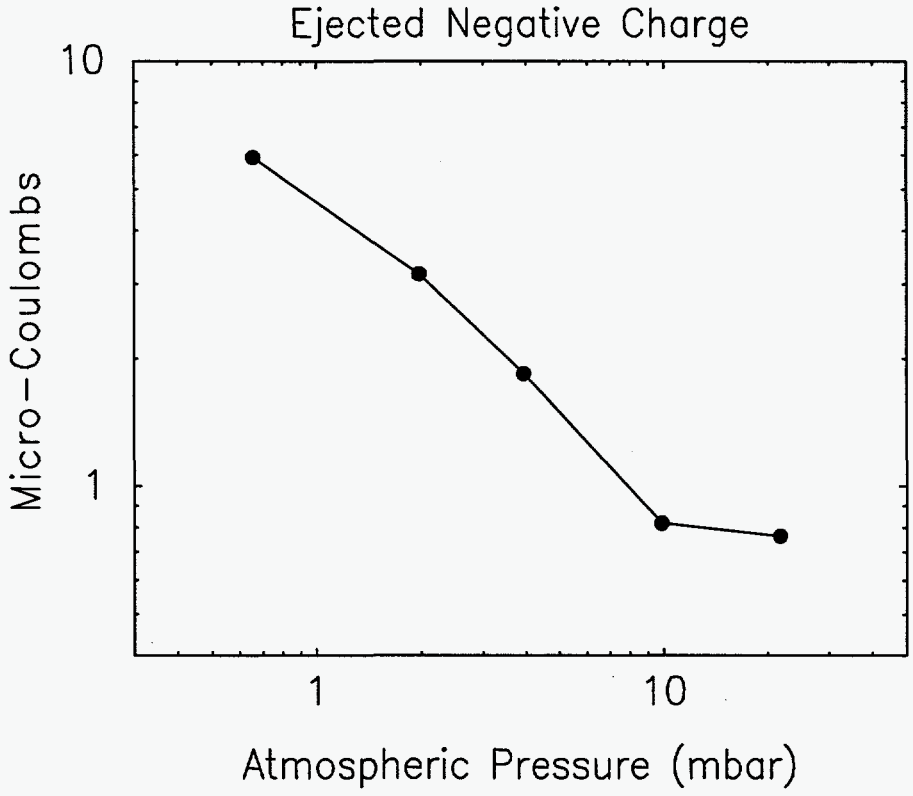

Fig. 8. Negative charge ejected by impacts of 0.48-cm spherical aluminum projectiles into granular carbonate (dolomite) targets at 4.8 km/s vs. atmospheric pressure.

The strength of the magnetic fields shown in Table 2 are only significant for the larger impact events. The 0.03 tesla magnetic field strength during a 1 km asteroid impact is about 1,000 times greater than Earth's natural surface field strength. Of course, due to the mechanism of 'dust discharge' suggested above, fields of this strength may not occur during actual events, but fields comparable to Earth's are perhaps possible. The magnetic field could last 100's of seconds, comparable to the crater formation time, and perhaps long enough for materials transported, shocked and heated by the impact to acquire a remnant magnetization.

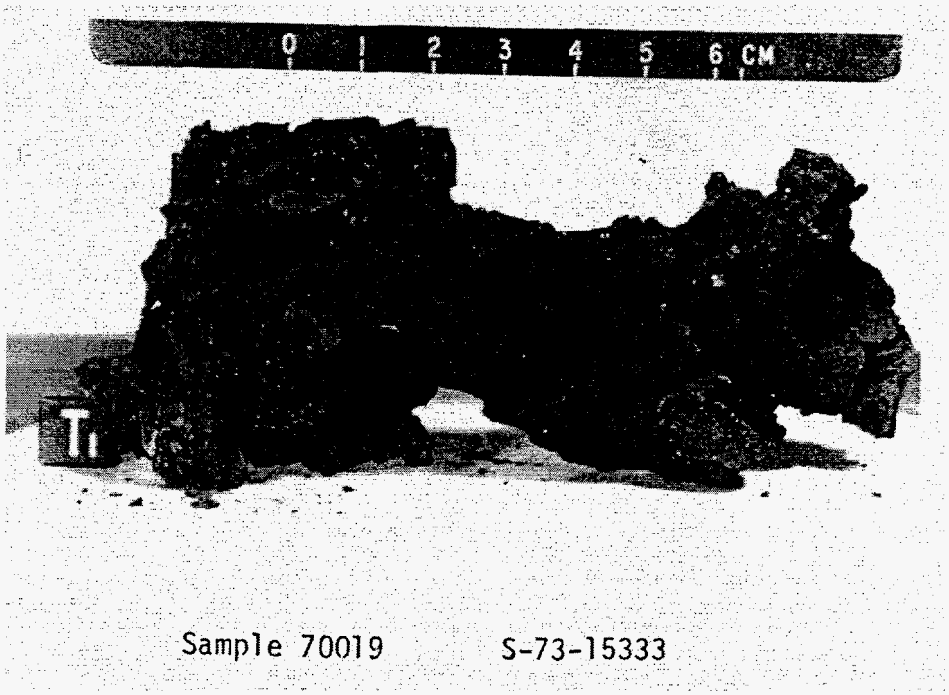

Fig. 9. Sample 70019 collected during Apollo 17 from the bottom of a 3-m glass-lined crater (Fig. 10). It was collected as a good candidate for obtaining a magnetic paleointensity estimate of the landing site.

It has been known since Apollo that the Moon possesses a patchy remnant magnetism associated predominantly with heavily cratered terrain [8]. There are two generally accepted possibilities for the origin of this magnetism: 1) that the Moon originally possessed an internal core dynamo field which is retained today in a heavily modified state by the older regions of the lunar surface or 2) that some, if not all, of the remnant magnetism may be due to spontaneous production by impacts. The recent arrival of Lunar Prospector, with magnetic mapping among its many tasks, may finally answer this question. We suggest that macroscopic charge separation and subsequent magnetic field production during hypervelocity impact may play an important role in understanding the lunar magnetic record.

Sample 70019 (Figure 9), was collected from the bottom of a 3-m glass pit crater (Figure 10) in the hope that it would provide a relatively recent magnetic paleointensity value for the Apollo 17 landing site [9]. It is a glass-bonded agglutinate of a dark, weakly coherent breccia, presumably formed by the impact that made the crater. A paleomagnetic experiment conducted by Sugiura et al. [10] demonstrated that sample 70019 (or more accurately, its glassy rind) was formed in a magnetic field of ~2500 nT, which is almost ten times stronger than the largest present-day field measured at the lunar surface. Because the young age of the sample (3 to 200 million years) precludes an ancient core dynamo origin for the magnetic field, this is a good candidate for a magnetic field formed by hypervelocity impact. We estimate that a 1-5 kg meteoroid impacting the lunar surface at 15 km/s would, in the process of making a 3-m crater, produce a several thousand nanotesla field for 4-8 milliseconds (Example 3 in Table 2), long enough for small beads of impact melt to acquire a permanent magnetic remanence.

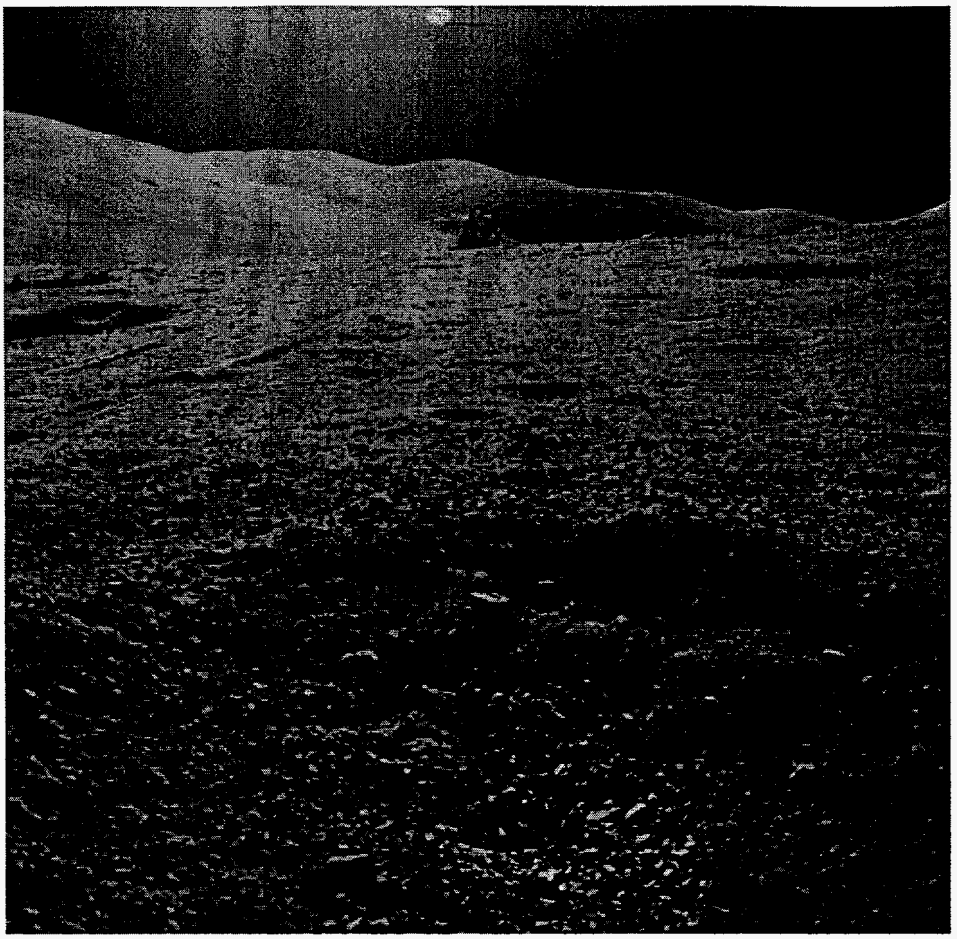

Fig. 10. A 3-m impact crater observed by the astronauts of Apollo 17. Sample 70019 was collected from the central glass-lined pit at the extreme foreground of the image (NASA photograph AS17-145-22185).

CONCLUSION

The production of a charged debris environment during hypervelocity impact is inevitable. A straightforward experimental technique, using conducting plates connected to digitizing electronics, can measure the degree of charge separation and map out the spatial extent and velocity distribution of the charged debris. In this study, we have demonstrated that the amount of plasma, electrostatic charge and the magnitude of the resulting currents and electric fields have near linear dependence on impactor mass and near cubic dependence on the impact velocity ($\propto v^{2.6}$). A straightforward extrapolation for microscopic Leonid meteoroids impacting spacecraft at 72 km/s, suggests that electric currents from potential discharges may approach several amps, levels that could be dangerous to spacecraft electronics. The resulting magnetic fields, while insignificant at microscopic and laboratory scales, increase linearly with impactor radius and can potentially explain the otherwise puzzling paleomanetic field determined for at least one young lunar sample and can help our more general understanding of the paleomagnetism of the Moon, Mars, asteroids and other planetary surfaces.

Acknowledgements—The authors would like to thank the NASA Ames Vertical Gun Crew: John Vongray, Wayne Logsdon and Ben Langedyk for their assistance in performing the experiments. Sandia is a multiprogram laboratory operated by Sandia Corporation, a Lockheed Martin Company, for the United States Department of Energy under Contract DE-AC04-94AL85000.

REFERENCES

1. D. A. Crawford and P. H. Schultz, Laboratory observations of impact-generated magnetic fields, *Nature*, **336**, 50-52 (1988).
2. D. A. Crawford and P. H. Schultz, Laboratory investigations of impact-generated plasma, *J. Geophys. Res.*, **96** (E3), 18,807-18,817 (1991).
3. D. A. Crawford and P. H. Schultz, The production and evolution of impact-generated magnetic fields, *Int. J. Impact Engng.*, **14**, 205-216 (1993).
4. L. L. Hood and A. Vickery, Magnetic field amplification and generation in hypervelocity meteoroid impacts with application to lunar paleomagnetism, *Proc. Lunar Planet. Sci. Conf. 15, J. Geophys. Res.*, **89** (suppl.), C211-C223 (1984).
5. R. D. Caswell, N. McBride and A. Taylor, Olympus end of life anomaly – a Perseid meteoroid impact event?, *Int. J. Impact Engng.*, **17**, 139 (1995).
6. M. M. Campbell and D. F. Medina, Kinetic Damage to External Satellite Materials due to the Impact of Leonid Micrometeoroids in the 10 Microgram Mass Range, presented at the Leonid Meteoroid Storm and Satellite Threat Conference, Manhattan Beach, CA, April, (1998).
7. H. Dietzel, G. Neukum and P. Rauser, Micrometeoroid Simulation Studies on Metal Targets, *J. Geophys. Res.*, **77**, 1375-1395 (1972).
8. M. Fuller, Lunar Magnetism, *Reviews of Geophys. And Space Phys.*, **12**, 23-70 (1974).
9. Apollo 17 Preliminary Examination Team, Apollo 17 Lunar Samples: Chemical and Petrographic Description, *Science*, **182**, 659-672 (1973).
10. N. Sugiura,. *et al.*, A new magnetic paleointensity value for a "young lunar glass", *Proc. Lunar Sci. Conf.*, **10**, 2189-2197 (1979).